LIMNOLOGY
and
OCEANOGRAPHY: METHODS

ASLO

*Limnol. Oceanogr.: Methods* 00, 2016, 00–00

doi: 10.1002/lom3.10137

# Spectrophotometric measurement of freshwater pH with purified meta-cresol purple and phenol red

**Chun-Ze Lai,[1] Michael D. DeGrandpre,*[1] Brandon D. Wasser,[1] Taymee A. Brandon,[1] Daniel S. Clucas,[1] Emma J. Jaqueth,[1] Zachary D. Benson,[1] Cory M. Beatty,[1] Reggie S. Spaulding[2]**

[1]Department of Chemistry and Biochemistry, University of Montana, Missoula, Montana
[2]Sunburst Sensors, Missoula, Montana

## *Abstract*

Impurities in indicator salts can significantly bias spectrophotometric pH determinations. In this work, two purified sulfonephthalein indicators, meta-cresol purple (mCP) and phenol red (PR), were tested for analysis of freshwater pH on the free hydrogen ion concentration scale. These two purified indicators were characterized for the first time under low ionic strength conditions, providing their molar absorption coefficients and dissociation constants along with their temperature dependence from 8 °C to 30 °C. At 25 °C, the infinite dilution constants ($pK_I^o$) were determined to be 8.6606 and 8.0642 for mCP and PR, respectively. The accuracy and precision of the method, evaluated with a variety of buffers with known pH, were found to be +0.0014 pH units and ±0.0022 pH units, respectively ($n = 30$). The pH values of different freshwater samples were also determined using both indicators. The mCP and PR results were all within ± 0.01 pH units of each other with three out of seven pH differences within ± 0.001 pH units, indicating the high consistency between these two indicator methods. The work presented here is the first parallel comparison with two purified indicators used to determine pH of the same freshwater samples.

Spectrophotometric pH has long been the preferred method for pH analysis of seawater because of its innate reproducibility and excellent precision (Byrne and Breland 1989; Clayton and Byrne 1993; DeGrandpre et al. 2014). Widespread acceptance of the method was preceded by careful characterization of the optical and thermodynamic properties of sulfonephthalein indicators in a seawater matrix (Robert-Baldo et al. 1985). There have been similar efforts to characterize these indicators for freshwater analysis (Yao and Byrne 2001; French et al. 2002; Yuan and DeGrandpre 2008) and for other low ionic strength solutions (Yamazaki et al. 1992; Raghuraman et al. 2006). However, most freshwater studies and monitoring programs continue to rely on glass pH electrodes. For example, the U.S. Geological Survey still uses glass electrodes for their extensive water quality monitoring program (Butman and Raymond 2011) and many limnological research programs use pH electrode measurements (Talling 2010; Wallin et al. 2010; Nimick et al. 2011). While these measurements provide long-term methodological consistency, the uncertainty in pH due to liquid junction and other errors (Davison and Woof 1985; Stauffer 1990), and the inherent drift and the need to frequently calibrate pH electrodes, limit the usefulness of pH electrode data for discerning long-term trends and computing inorganic carbon and other chemical speciation in freshwater systems (French et al. 2002; Martz et al. 2003; Abril et al. 2015).

The freshwater spectrophotometric pH method can enhance the utility of pH data for many different applications but further validation is needed. In Yao and Byrne (2001), the $pK_I^o$s for bromocresol purple and phenol red (PR) were determined at infinite dilution and excellent precision was obtained for river water (±0.001 pH units) but there was no assessment of accuracy. French et al. (2002) measured the pH of dilute phosphate buffers and river water with cresol red after determining the equilibrium constant. The measurements compared to within 0.003 ± 0.008 pH units of the buffer pH. Yuan and DeGrandpre (2008) evaluated the dependence of buffer intensity on the pH perturbation of freshwater using cresol red and bromothymol blue. None of these studies have compared different indicators for analysis of the same sample. This comparison could provide valuable insights into the accuracy of the method. Additionally, none of the previous freshwater work has utilized purified sulfonephthalein indicators. Indicator impurities have been found to cause significant seawater pH errors (Yao et al. 2007; Liu et al. 2011; Patsavas et al. 2013), and have led to use of

*Correspondence: michael.degrandpre@umontana.edu

purified indicators for seawater pH analysis (Liu et al. 2011; DeGrandpre et al. 2014). It is unknown to what extent the impurities could affect freshwater pH accuracy, but it is worthwhile to obtain accurate "impurity-free" thermodynamic and optical properties of the indicators for future applications.

In this work, we have purified meta-cresol purple (mCP) and PR and have quantified their molar absorption coefficients and $pK_I^o$ at low ionic strengths. The indicator mCP was selected because we have purified mCP available for our seawater applications; whereas, PR was selected because its $pK_I^o$ is optimal for freshwater analysis and is close enough to the $pK_I^o$ of mCP that comparisons can be made. Here, the two indicators are used to analyze a wide range of low ionic strength samples, including weak buffers and a variety of natural water samples.

## Theory

The spectrophotometric pH method, which is used in this work, is based on the equilibrium of a weak diprotic acid indicator:

$$HI^- \leftrightarrow H^+ + I^{2-} \tag{1}$$

where $HI^-$ is the protonated (acid) form and $I^{2-}$ is the deprotonated (base) form. The second dissociation constant of the indicator is

$$K_I = \frac{[H^+][I^{2-}]}{[HI^-]} \cdot \frac{\gamma_{H^+}\gamma_{I^{2-}}}{\gamma_{HI^-}} \tag{2}$$

where $\gamma$ denotes activity coefficient. The pH, determined on the free hydrogen ion concentration scale, is expressed as:

$$pH = -\log[H^+] = pK_I^o + \log\left(\frac{R - e_1}{e_2 - Re_3}\right) + \log\frac{\gamma_{H^+}\gamma_{I^{2-}}}{\gamma_{HI^-}} \tag{3}$$

where $R$ is the ratio of indicator absorbances at the absorbance maxima of $I^{2-}$ and $HI^-$. For mCP, $\lambda_1 = 434$ nm and $\lambda_2 = 578$ nm, and for PR, $\lambda_1 = 433$ nm and $\lambda_2 = 558$ nm for $HI^-$ and $I^{2-}$, respectively. $pK_I^o$ is the negative logarithm of the second dissociation constant of the indicator at zero ionic strength. The term $(R - e_1)/(e_2 - Re_3)$ is equal to the ratio $[I^{2-}]/[HI^-]$, where $e_1$, $e_2$, and $e_3$ refer to molar absorption coefficient ratios corresponding to $HI^-$ or $I^{2-}$ at $\lambda_1$ or $\lambda_2$:

$$e_1 = \frac{\varepsilon_{HI,\lambda_2}}{\varepsilon_{HI,\lambda_1}} \quad e_2 = \frac{\varepsilon_{I,\lambda_2}}{\varepsilon_{HI,\lambda_1}} \quad e_3 = \frac{\varepsilon_{I,\lambda_1}}{\varepsilon_{HI,\lambda_1}} \tag{4}$$

After the determination of $e_i$s and $pK_I^o$ (described below), the pH on the free hydrogen ion concentration scale can be obtained using:

$$pH = pK_I^o + \log\left(\frac{R - e_1}{e_2 - Re_3}\right) - 4A\left(\frac{\sqrt{\mu}}{1 + \sqrt{\mu}} - 0.3\mu\right) \tag{5}$$

where $\mu$ is the ionic strength and

$$A = 0.5092 + (T - 298.15) \times 8.5 \times 10^{-4} \tag{6}$$

where $T$ is the temperature in Kelvin. Equation 5 can be used for ionic strengths $\leq 0.05$ M.

## Materials and procedures

### Materials

Indicators mCP (Lot No. 11517KCV, 90 wt%) and PR (Lot No. 13912PS, 95 wt%) were purchased from Sigma-Aldrich (St. Louis, MO) and purified before use (see below). The buffers used in this work ($CH_3COOH$, $Na_2HPO_4$, $KH_2PO_4$) were analytical grade and obtained from Fluka (Buchs, Switzerland) and Mallinckrodt Baker (Paris, KY). Certified standard solutions of 0.1 N HCl and 0.1 N NaOH were purchased from Fisher Scientific (Pittsburgh, PA). Acetonitrile (HPLC grade) was obtained from Fisher Scientific and trifluoroacetic acid was obtained from Sigma-Aldrich. Nanopure water (17.9 MΩ·cm specific resistance), obtained with a Barnstead water purification system (Thermo Scientific, Waltham, MA), was used for all solutions.

The mCP and PR stock solutions used for pH analyses had concentrations of $9.25 \times 10^{-4}$ mol·kg soln$^{-1}$ and $1.25 \times 10^{-3}$ mol·kg soln$^{-1}$, respectively. To minimize the perturbation of the sample pH, each of the indicator solutions was adjusted to a pH of ~7.5 with a 0.1 N HCl or 0.1 N NaOH solution while being monitored with an Orion combination pH electrode connected to a dual channel pH/ion meter (Accumet™, model AR25, Fisher Scientific).

Phosphate buffer salts $Na_2HPO_4$ and $KH_2PO_4$ were dried at 105 °C for 2 h before weighing. The solutions were prepared using Nanopure water that was degassed by boiling under vacuum. The acid component of the buffer ($KH_2PO_4$) was first added to water with approximately half total solvent volume to prevent $CO_2$ contamination at dissolution. The base component ($Na_2HPO_4$) was then added and the flask was filled to the final volume. Buffer solutions were purged with $N_2$ gas in the head-space when transferred to a Nalgene bottle for storage.

### Purification of mCP and PR

Indicators mCP and PR were purified with a flash chromatography system (CombiFlash® Rf, Teledyne ISCO, Lincoln, NE) (Liu et al. 2011; Patsavas et al. 2013). The reversed phase C-18 column (C18Aq, Teledyne ISCO) was loaded with ~1 g mCP or PR dissolved in a 100 mL of solvent containing water, acetonitrile and trifluoroacetic acid (95.0 : 5.0 : 0.05, v : v : v). The purified indicators were eluted during a gradient that increased the acetonitrile from 5% to 40% for mCP or to 45% for PR. The eluent was captured in sequential test tubes and then combined and dried at room temperature in a stoppered flask with ultrapure air blown onto the solution. The air-dried sample was then dried at 35 °C and 15 mm Hg vacuum for 2 h. The typical yield was 50–60% for both mCP and PR. After purification, based on the change in the ratio

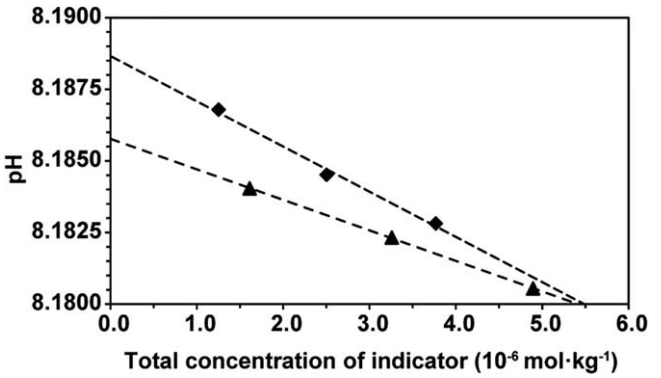


**Fig. 1.** Effect of total indicator concentration (◆ for mCP and ▲ for PR) on the measured pH. Data shown in the figure were collected by sequential addition of indicator to a Clark Fork River sample. The *y*-intercept is assumed to be the true sample pH where no indicator is present.

of peak areas of the contaminants to the peak area of the indicator, 96.4% of contaminants were removed from mCP, resulting in a purity of 99.7%, and 86.0% of contaminants were removed from PR, resulting in a purity of 99.3%.

**Spectrophotometric measurements**

All spectrophotometric measurements were carried out on a benchtop spectrophotometer (Cary 300, Varian) with a 10 cm path length, capped, quartz cuvette. The performance of the spectrophotometer was routinely checked with wavelength and absorbance standards (DeGrandpre et al. 2014). The solution temperature was controlled with a water-jacketed spectrophotometric cell holder. The actual temperature of the indicator solution in the cuvette was measured by a high accuracy temperature probe (Eutechnics, 15-060-381, Fisher Scientific), immersed in the sample via a hole drilled in the cell stopper. Before measurement, sample bottles were placed in a water bath set to the approximate measurement temperature. After ~20 min temperature equilibration, the cuvette, containing a stir bar, was filled with sample, capped, wiped dry, and placed in the spectrophotometer. A magnetic stirring wand was mounted to the upper wall of the cell holder to mix the indicator without removing the cell. Light absorption was measured at the absorbance maxima and at 780 nm (to account for offsets between the blank and sample). Absorbance offsets at 780 nm were typically $< 0.002$ absorbance units (a.u.).

As stated in the introduction section, indicators themselves are weak acids or bases. A pH change of $< 0.005$ pH units due to addition of the indicator is typical for seawater samples (Chierici et al. 1999). Because freshwaters usually have lower buffer intensity, the effect of the indicator on the pH can be more pronounced (Yuan and DeGrandpre 2008). Consequently, for freshwater analyses, the pH perturbation should be determined for every sample to obtain the best accuracy. To determine the perturbation-free pH value, a solution of mCP or PR is sequentially added to the sample. We typically add 40 $\mu$L of stock indicator solution for each of three additions, corresponding to an indicator concentration range from $1.2 \times 10^{-6}$ mol·kg soln$^{-1}$ to $3.7 \times 10^{-6}$ mol·kg soln$^{-1}$ for mCP and $1.6 \times 10^{-6}$ mol·kg soln$^{-1}$ to $5.0 \times 10^{-6}$ mol·kg soln$^{-1}$ for PR and an absorbance range from 0.5 to 1.5 a.u. The total concentration of indicator in the sample solution is calculated and plotted along with the calculated pH (Fig. 1). The *y*-intercept, where no indicator is present, is assumed to be the true pH, or perturbation-free pH, for the sample (French et al. 2002). The SAMI-pH sensor technology uses an automated form of this methodology (Martz et al. 2003; Seidel et al. 2008).

**Indicator characterization**

For mCP, an acetic acid solution with pH ~4.4 was used to determine the molar absorption coefficient of $HI^-$ at 434 nm and 578 nm. At this pH, the presence of the other two forms ($H_2I$) and ($I^{2-}$) is minimized (their concentrations are about $10^4$ times lower than [$HI^-$]). Higher or lower pH would increase the absorbance of the other two forms, causing inaccurate determination of molar absorption coefficient of [$HI^-$]. For PR, similarly, an acetic acid solution with pH 4.4 was used to determine the molar absorption coefficient of $HI^-$ at 433 nm and 558 nm. A 0.01 M NaOH solution with pH 12 was used to determine the molar absorption coefficients of $I^{2-}$ for mCP and PR at 434 nm and 578 nm, and 433 nm and 558 nm, respectively. The molar absorption coefficients were measured at four temperatures, ~8, 17, 22 and 30 °C. The molar absorption coefficients at these ionic strengths ($\leq$0.010 M) are not expected to differ significantly from ionic strengths over the freshwater range because others have shown the salinity dependence is weak (DeGrandpre et al. 2014). It should also be noted that, while being stored in the dark, the absorbance intensity of mCP at pH 12 degraded by 0.0005 a.u./d for a 10 cm cell. Therefore, we prepared fresh pH 12 indicator solutions to minimize the error in measurements if the experiments spanned more than 1 d.

As shown in Eq. 3, the pH measurement accuracy directly depends on the accuracy of $pK_I^o$. However, $pK_I^o$ values for purified mCP and PR under low ionic strength conditions have not been reported. Therefore, $pK_I^o$ and its temperature dependence were determined in this work by adding indicator to phosphate buffers with known pH. The $pK_I^o$ was then calculated using the following equation (Yao and Byrne, 2001):

$$pK_I^o = pK_2^o - \log \frac{[H_2PO_4^-]}{[HPO_4^{2-}]} - \log\left(\frac{R - e_1}{e_2 - Re_3}\right) \quad (7)$$

where $pK_2^o$ is the negative logarithm of second dissociation constant of the phosphate buffer (Bates and Acree 1943). The actual concentrations of $H_2PO_4^-$ and $HPO_4^{2-}$ for use in Eq. 7 were calculated using an in-house program written in Visual Basic in Excel. Since the typical freshwater ionic strength is between 0 and 0.005 M (Domenico and Schwartz

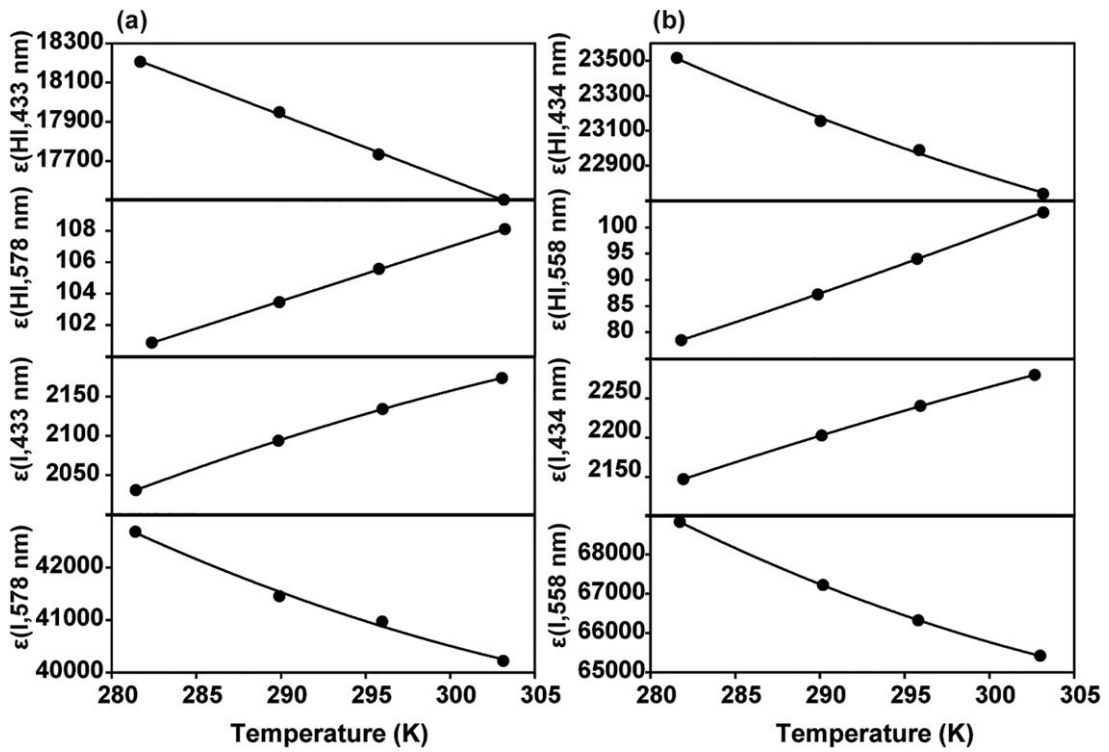


**Fig. 2.** Temperature dependence of the molar absorption coefficients measured using purified (**a**) mCP and (**b**) PR at the wavelengths of maximum absorption for each chemical species.

1990; Pankow 1991), the ionic strengths of diluted phosphate buffer used for the $pK_I^o$ determination were all $\leq 0.010$ M.

**pH accuracy evaluation**

The accuracy of the pH determined with mCP and PR was evaluated by measuring the pH of a series of phosphate buffers. The actual pH values of these buffers were known through the calculation using the in-house equilibrium program that includes the temperature dependence of $pK_w$ (the negative logarithm of the water ion product) (Millero 2007) and $pK_2^o$ of the phosphate buffer. The pH values were measured over a wide temperature range (8–30 °C). Ionic strengths for all phosphate buffers were approximately 0.010 M. An independent accuracy evaluation was also carried out by determining pH values of a borate buffer (ionic strength was ~0.010 M) repeatedly with both mCP and PR.

**pH of freshwater samples**

Different freshwater samples, including tap water, and samples collected during several field visits to local streams including Rattlesnake Creek, Blackfoot River, Clark Fork River near Gold Creek (labeled as Gold Creek) and near Missoula (labeled as Missoula), were also analyzed with both indicators. Samples were kept in the dark to limit any possible alteration of the sample and were typically analyzed within 4 h. Samples were used directly without filtering to avoid the change of pH due to $CO_2$ exchange in the procedure. Freshwater samples were tested back to back, e.g., one sample with mCP followed by one sample with PR, or in the opposite order. Measurements were carried out on temperature-equilibrated samples with three sequential additions of 40 $\mu$L of indicator stock solution as described above (see Fig. 1). All freshwater samples were measured at 25 °C.

## *Assessment*

**Molar absorption coefficients and ratios**

With the successful purification of indicators in this work, the molar absorption coefficients for mCP and PR could be accurately determined at low ionic strength for the first time. Figure 2 shows the temperature dependence of the molar absorption coefficients at the wavelengths of maximum absorption for both mCP and PR. The molar absorption coefficients decrease with increasing temperature at the absorbance maxima for acid and base forms for both mCP and PR. Conversely, for the molar absorption coefficients that are not at the absorbance maxima (i.e., $\varepsilon_{HI^-,578}$ and $\varepsilon_{I^{2-},434}$ for mCP, and $\varepsilon_{HI^-,558}$ and $\varepsilon_{I^{2-},433}$ for PR), the molar absorption coefficients increase with increasing temperature for both mCP and PR. These trends have been observed before and are due to both a slight spectral shift to longer wavelengths in the $I^{2-}$ peaks and to shorter wavelengths for the $HI^-$ peaks (Harris 2013).

**Table 1.** Molar absorption coefficients for mCP and PR and their temperature dependence at the analytical wavelengths.

| Indicator | Fitted equation* | $r^2$ | Residual | $\varepsilon$ at 25 °C ($M^{-1}$ $cm^{-1}$)† |
|---|---|---|---|---|
| mCP | $\varepsilon_{HI^-,434} = -4.6960 \times 10^{-3}T^2 - 3.0214 \times 10^{1}T + 2.7092 \times 10^{4}$ | 0.99904 | $0.00 \pm 9.3$ | 17,666 |
| | $\varepsilon_{HI^-,578} = -1.1158 \times 10^{-4}T^2 + 4.1248 \times 10^{-1}T - 6.7050$ | 0.99986 | $0.0 \pm 3.6 \times 10^{-2}$ | 106 |
| | $\varepsilon_{I^{2-},434} = -6.7456 \times 10^{-2}T^2 + 4.6026 \times 10^{1}T - 5.5793 \times 10^{3}$ | 1.0000 | $1.7 \times 10^{-1} \pm 8.7 \times 10^{-2}$ | 2147.0 |
| | $\varepsilon_{I^{2-},578} = 1.5877T^2 - 1.0392 \times 10^{3}T + 2.0937 \times 10^{5}$ | 0.99484 | $1.4 \times 10^{1} \pm 7.4 \times 10^{1}$ | 40,669 |
| PR | $\varepsilon_{HI^-,433} = 3.4018 \times 10^{-1}T^2 - 2.3446 \times 10^{2}T + 6.2560 \times 10^{4}$ | 0.99762 | $0.0 \pm 1.6 \times 10^{1}$ | 22,896 |
| | $\varepsilon_{HI^-,558} = 4.1299 \times 10^{-3}T^2 - 1.2731T + 1.0929 \times 10^{2}$ | 0.99999 | $1.1 \times 10^{-2} \pm 3.4 \times 10^{-2}$ | 96.836 |
| | $\varepsilon_{I^{2-},433} = -3.5570 \times 10^{-2}T^2 + 2.7201 \times 10^{1}T - 2.6943 \times 10^{3}$ | 0.99996 | $8.9 \times 10^{-2} \pm 3.5 \times 10^{-1}$ | 2253.7 |
| | $\varepsilon_{I^{2-},558} = 2.3897T^2 - 1.5575 \times 10^{3}T + 3.1796 \times 10^{5}$ | 0.99997 | $-1.3 \times 10^{1} \pm 7.4$ | 66,020 |

*The temperature is in Kelvin.
†$M^{-1}$ $cm^{-1}$ = 100 $M^{-1}$ $m^{-1}$.

The fitted equations for data shown in Fig. 2 are listed in Table 1 along with the $r^2$, mean residual and standard deviation. In addition, molar absorption coefficients for both mCP and PR at 25 °C are listed as examples. The molar absorption coefficient ratios, $e_i$s, for mCP and PR were then calculated according to Eq. 4 using the actual data. Because it is critical to account for the $e_i$ temperature dependence (DeGrandpre et al. 2014), the $e_i$ temperature dependence along with the $r^2$ and mean residuals are shown in Table 2. The $e_i$ values for mCP and PR at 25 °C are also listed as examples.

### Indicator p$K_I^o$

Figure 3 shows the results of the p$K_I^o$ determination using the phosphate buffers and includes the best fit curves and residuals. The temperature dependence of p$K_I^o$ for both mCP and PR exhibits the same trend of decreasing p$K_I^o$ with increasing temperature. This relationship is due to endothermic acid dissociation reactions that are more favorable at higher temperature. Both mCP and PR data are accurately fitted with an equation of the form $pK_I^o = A + BT + \frac{C}{T} + D\ln T$. The mean residuals are indiscernible from zero (Table 3) with no clear trend with temperature (Fig. 3). The p$K_I^o$s for unpurified PR calculated using the equations in Yao and Byrne (2001) follow the same trend but are lower than the corresponding p$K_I^o$s for purified PR. Table 3 lists the p$K_I^o$ equations for purified mCP and PR between 8 °C and 30 °C. With these equations, p$K_I^o$ at 25 °C is 8.6606 for mCP and 8.0642 for PR, respectively. For comparison, p$K_I^o$ at 25 °C for unpurified PR at zero ionic strength is 8.0341 (Yao and Byrne 2001). The lower p$K_I^o$ for unpurified PR could be the result of several different factors; for example, the impurities in PR could deprotonate at a lower pH or they could bias the determination of the $e_i$ values and therefore the p$K_I^o$ determined using Eq. 7.

### Accuracy evaluations

After determining the p$K_I^o$s, we used a phosphate buffer with pH different from that used to determine the p$K_I^o$ but with 0.010 M ionic strength to evaluate the accuracy of the method over a range of temperatures. As shown in Fig. 4, the pH values with the purified indicators match well with the calculated pH of the phosphate buffers in the temperature range 8–30 °C. The pH values only slightly deviate from the 1 : 1 line. For mCP, the average absolute residual is $0.0016 \pm 0.0009$ pH units ($n = 12$) and the maximum residual is 0.0026 pH units, and for PR, the average absolute residual is $0.0016 \pm 0.0013$ pH units ($n = 9$) and the maximum residual is 0.0040 pH units. These small pH errors confirm the high accuracy of the spectrophotometric method with purified mCP and PR under low ionic strength conditions. Notably, mCP performed as well as PR even though its p$K_I^o$ is considered "out of range," i.e., the pH of some of the samples were not within the p$K_I^o$ ± 1 range. In this case, the molar absorption coefficient of the base form of mCP is about twice of that of acid form (Table 1); therefore, there is still sufficient absorbance to obtain good accuracy and precision at the low pHs (Fig. 4). It is also evident from Fig. 4 that most pH values with both mCP and PR are slightly higher than the actual pH value. There are also systematic deviations at the extreme ranges of temperature and pH for the PR analyses (Fig. 4 middle and right panels). The reasons for these small positive errors are not clear.

These tests also show that the spectrophotometric pH method has very high precision. The average standard deviation for all pH values at different temperatures is ± 0.0006 for both mCP and PR ($n = 21$). Furthermore, five additional buffer measurements with mCP were carried out at 25.19 ± 0.08 °C and the standard deviation is ± 0.0008.

The accuracy of pH measurements with purified mCP and PR was more directly assessed by measuring phosphate buffers with both pH (ranging from 7.520 to 8.131) and ionic strength (ranging from 0.0050 M to 0.0100 M) that differed from that used to determine p$K_I^o$ (Table 4). The larger uncertainties were not due to the spectrophotometric pH measurement because mCP and PR matched to within $-0.0009 \pm 0.0082$ pH units for these samples. These results support the findings of Yuan and DeGrandpre (2008) that accuracy and precision degrade with lower buffer intensity;

**Table 2.** Molar absorptivity ratios ($e_i$s) (Eq. 4) and their temperature dependence.

| | Fitted equation* | $r^2$ | Residual | $e$ at 25 °C |
|---|---|---|---|---|
| *mCP* | | | | |
| $e_1$ | $e_1 = 1.5036 \times 10^{-7}T^2 - 5.8331 \times 10^{-5}T + 1.0044 \times 10^{-2}$ | 0.99968 | $0.0 \pm 0.0$ | 0.006 |
| $e_2$ | $e_2 = 3.1400 \times 10^{-5}T^2 - 2.0527 \times 10^{-2}T + 5.6349$ | 1.0000 | $-3.2 \times 10^{-3} \pm 6.7 \times 10^{-3}$ | 2.306 |
| $e_3$ | $e_3 = -2.8764 \times 10^{-6}T^2 + 2.2697 \times 10^{-3}T - 2.9948 \times 10^{-1}$ | 0.99982 | $-1.4 \times 10^{-5} \pm 7.2 \times 10^{-5}$ | 0.1215 |
| *PR* | | | | |
| $e_1$ | $e_1 = 2.6445 \times 10^{-7}T^2 - 9.9420 \times 10^{-5}T + 1.0361 \times 10^{-2}$ | 1.0000 | $0.0 \pm 0.0$ | 0.004 |
| $e_2$ | $e_2 = 6.2236 \times 10^{-5}T^2 - 3.8762 \times 10^{-2}T + 8.9077$ | 0.99225 | $0.0 \pm 1.9 \times 10^{-3}$ | 2.883 |
| $e_3$ | $e_3 = -3.0956 \times 10^{-6}T^2 + 2.2264 \times 10^{-3}T - 2.9019 \times 10^{-1}$ | 0.99992 | $-6.2 \times 10^{-6} \pm 3.4 \times 10^{-5}$ | 0.0984 |

*The temperature is in Kelvin.

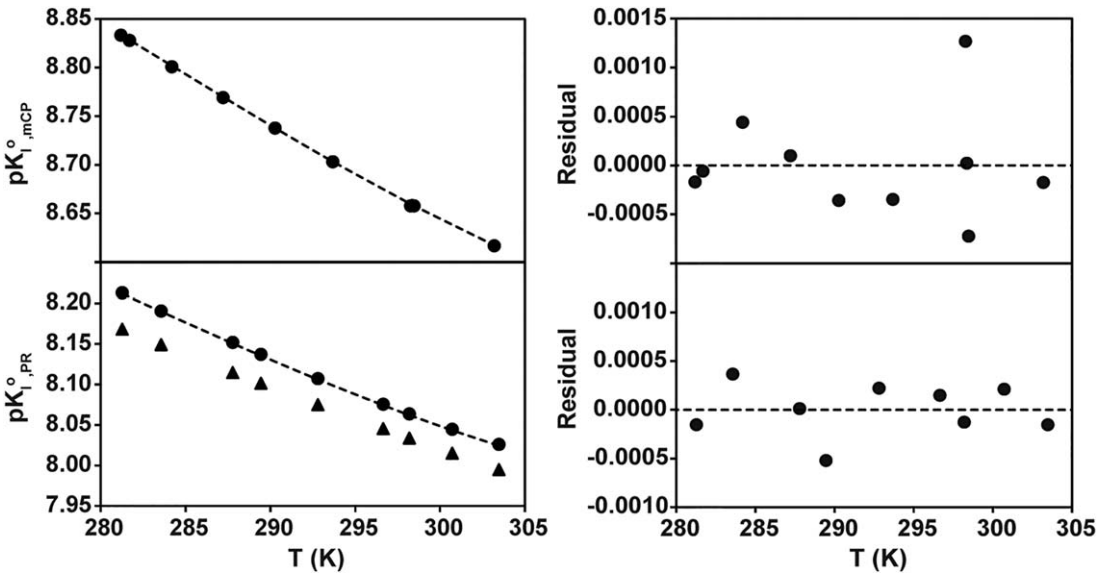


**Fig. 3.** Temperature dependence of the dissociation constants for purified mCP (top) and PR (bottom) along with residuals (fitted p$K_I$° – measured p$K_I$°) of the fit (right). For comparison, the p$K_I$°s for unpurified PR predicted with the equation by Yao and Byrne (2001) are also shown (▲).

**Table 3.** Temperature dependence of p$K_I$°.

| Indicator | Fitted equation for p$K_I$°* | $r^2$ | Residual | p$K_I$° at 25 °C |
|---|---|---|---|---|
| mCP | $pK_I^\circ = \frac{-5.0242 \times 104}{T} - 3.5433 \times 10^2 \ln T + 6.1409 \times 10^{-1} T + 2.0129 \times 10^3$ | 0.99993 | $0.0 \pm 5.4 \times 10^{-4}$ | 8.6606 |
| PR | $pK_I^\circ = \frac{-3.5326 \times 104}{T} - 2.5305 \times 10^2 \ln T + 4.4364 \times 10^{-1} T + 1.4360 \times 10^3$ | 0.99997 | $0.0 \pm 2.7 \times 10^{-4}$ | 8.0642 |

*The temperature is in Kelvin.

however, the results were also not as good as previously obtained with the 0.010 M phosphate buffer. This larger uncertainty might be due to techniques used by different analysts and reflect the challenge in reproducible preparation of the weak buffers.

Finally, as an additional accuracy assessment, a borate buffer with known pH (ionic strength = 0.010 M) (Bower and Bates 1955) was repeatedly analyzed. The borate pH was determined to be $8.3182 \pm 0.0019$ ($n = 5$) at an average temperature of 25.10 °C (actual pH = 8.3163) by mCP with an error of 0.0019 pH units, and $8.3181 \pm 0.0054$ ($n = 4$) at an average temperature of 25.02 °C (actual pH = 8.3170) by PR with an error of 0.0011 pH units. These two pH values only differ by 0.0008 pH units after correction for temperature, indicating the high consistency of measurements between purified mCP and PR.

### Determination of pH for different freshwater samples

The purified mCP and PR were used to determine the pH for different freshwater samples. The comparison of pH

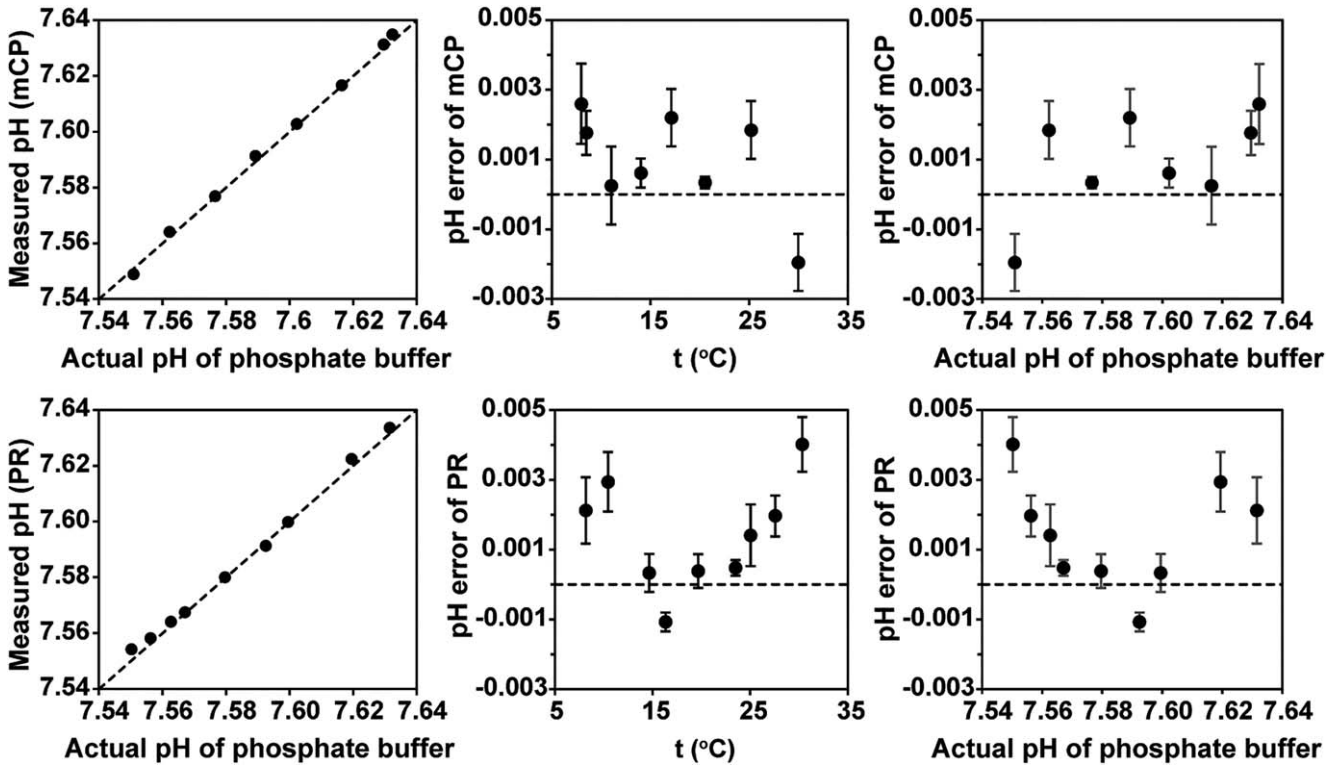


**Fig. 4.** pH of 0.010 M ionic strength phosphate buffers measured with purified mCP and PR (left panels, the dashed lines are the 1 : 1 relationships) and the calculated pH errors (measured pH – actual pH) for phosphate buffers at different temperatures (middle panels), and different buffer pH (right panels). The error bars indicate the standard deviation for the measured pH obtained from at least three replicates at the same temperature.

**Table 4.** Accuracy and precision for measurements of phosphate buffers with varied ionic strengths and pHs.

| Ionic strength (M) | Measured with mCP* | | Measured with PR* | |
|---|---|---|---|---|
| | pH error | SD | pH error | SD |
| 0.0100 ($n = 16$) | −0.0038 | 0.0074 | −0.0101 | 0.0067 |
| 0.0076 ($n = 16$) | −0.0243 | 0.0073 | −0.0235 | 0.0075 |
| 0.0050 ($n = 12$) | −0.0173 | 0.0280 | −0.0132 | 0.0268 |

*Data shown are based on four different pHs for 0.0100 M and 0.0076 M ionic strengths, and three different pHs for 0.0050 M ionic strength.

values for the two indicators is shown in Fig. 5 (top). Clearly, the determinations with purified mCP and PR provide highly comparable pH values for a wide range of sample types and pHs. To better visualize this, the pH differences are also shown in Fig. 5 (bottom). Their pH differences are all within ± 0.01 pH units. For three out of seven of the freshwater samples, the pH differences are within ± 0.001 pH units. The precision for the measurement in freshwater samples ranges from ± 0.0023 to ± 0.0162 pH units and ± 0.0033 to ± 0.0129 pH units for mCP and PR, respectively, and the mean standard deviation is ± 0.0082 pH units. Figure 5 also indicates that there is no systematic deviation with pH. The match between mCP and PR also implies that the two indicators have very similar ionic interactions in different ionic media, i.e., the activity coefficients are the same for both indicators. To our knowledge, this is the first reported parallel comparison with two purified indicators of different types for the same freshwater samples.

It also should be noted that the pH values for the freshwater samples do not include the activity coefficient contribution (see Eq. 5) due to the unknown sample ionic strength. We can, however, estimate the uncertainty due to this missing information. As reported previously (Yuan and DeGrandpre 2008), the mean ionic strength for Rattlesnake Creek was approximately $9 \times 10^{-4}$ M and therefore would shift the pH by −0.0588 pH units. The ionic strength for the Clark Fork River was estimated to be $5.3 \times 10^{-3}$ to $8.8 \times 10^{-3}$ M and would result in a shift of pH by −0.1350 to −0.1693 pH units (Lynch 2007). Because this correction is the same for mCP and PR, the resultant pH is the same. A ± 20% error in determination of ionic strength could result in −0.0056 to 0.0063 pH unit error for a low ionic strength environment (0.001 M) and −0.0113 to 0.0127 for a high ionic strength environment (0.005 M). To accurately determine the pH value of a freshwater sample, ionic strength should be quantified. The measurement of conductivity, e.g.,

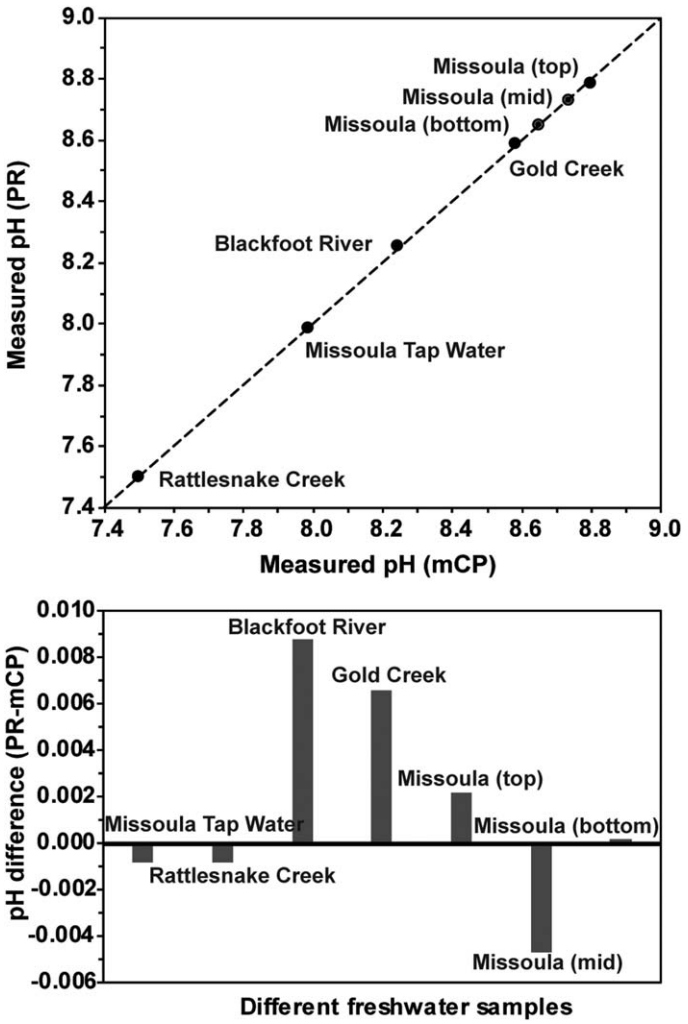


**Fig. 5.** Comparison of pH measured with both mCP and PR (top) and calculated pH differences for these data (bottom) for different samples.

using a conductivity meter such as Orion STAR Conductivity Meter (Thermo Scientific), is a rapid and inexpensive way of determining the ionic strength of a freshwater sample (Richards 1954) using the linear relationship between ionic strength and electrical conductivity (Griffin and Jurinak 1973).

**Discussions, implications, and recommendations**

The characterization of the purified indicators, mCP and PR, are reported under low ionic strength conditions for the first time. The spectrophotometric pH measurements with purified mCP and PR have high accuracy and precision based on analysis of phosphate and borate buffers with known pH. Furthermore, purified mCP and PR have been successfully used for measurement of different freshwater samples. The molar absorption coefficients and $pK_I^o$s can therefore be used in future studies to accurately measure pH if purified indicator is available and ionic strength is known. As shown in Fig. 1 and explained above, it is important to determine the perturbation-free pH for freshwater samples. For example, the pH for the Clark Fork River sample as determined by using mCP and PR is 8.1887 and 8.1858, respectively (Fig. 1). Under this specific circumstance, the fitting of the data finds that the perturbation of pH due to the addition of mCP or PR is $-1.58 \times 10^{-3}$ pH/($\mu$mol·kg$^{-1}$) and $-1.06 \times 10^{-3}$ pH/($\mu$mol·kg$^{-1}$), respectively. Therefore, theoretically, with the addition of 2.0 $\mu$mol·kg$^{-1}$ mCP or PR to this freshwater sample, the perturbations would be $-0.0032$ and $-0.0021$ pH units, respectively, for a 10 cm cell. When the experimental condition changes, including the pH of the sample, the buffer intensity of the sample, the pH of the indicator and the concentration of the indicator solution (e.g., 10X increase if using an optical pathlength of 1 cm), the extent of perturbation will also be changed. Consequently, the perturbation should be quantified for each analysis if accuracy better than 0.01 pH units is desired.

Future studies should include further validation of the equations in Tables 1, 2 with standard reference materials (e.g., those available from the U.S. National Institute of Standards and Technology). Spectrophotometric pH should also be combined with dissolved inorganic carbon or total alkalinity measurements on freshwater samples to verify that the partial pressure of $CO_2$ ($pCO_2$) can be accurately predicted using spectrophotometric pH. These studies are important because $pCO_2$ is commonly calculated using pH (from glass electrodes) and alkalinity (by titration) (Lynch et al. 2010; Butman and Raymond 2011; Finlay et al. 2015). These studies will establish the internal consistency of the spectrophotometric pH method like those completed for seawater pH (e.g., Clayton et al. 1995). Extension of the characterization of the purified indicators to estuarine conditions should also be conducted.

It is also important to note that, being an optical measurement, the optical transparency of the sample is important. The freshwater samples tested in this work were not filtered to avoid the change of pH due to $CO_2$ exchange. If necessary, samples could be filtered using a syringe with zero head space. The effect of suspended particulates or colored dissolved organic matter on measurements needs to be more systematically studied in the future. In addition, the spectrophotometric method with purified indicators, such as mCP and PR in the present work, can be used for direct calibration of glass pH electrodes in freshwater and evaluation of the electrode performance (Easley and Byrne 2012).

While freshwater pH is still primarily measured with pH electrodes due to their ease of use and low cost, the inaccuracy of these measurements reduces the pH's usefulness for geochemical modeling, especially for predicting inorganic carbon speciation. This work lays the foundation for future studies using spectrophotometric pH for long-term measurements of freshwater systems and combining the pH with

dissolved inorganic carbon or total alkalinity measurements on freshwater samples to accurately predict the inorganic carbon speciation. Although the spectrophotometric method may be more time-consuming and less portable, it is more reliable because the measurement is based on well-defined thermodynamic principles. Moreover, the challenge in sample handling, i.e., the sample needs to be put into a small cuvette where $CO_2$ exchange is more possible and temperature is difficult to measure and control, can be minimized if it is done carefully as demonstrated in this work. In addition, the spectrophotometric method can be made autonomous, as shown with the SAMI-pH (Martz et al. 2003; Spaulding et al. 2014), providing drift free, accurate, long-term monitoring for freshwater systems.

## REFERENCES


Abril, G., and others. 2015. Large overestimation of $pCO_2$ calculated from pH and alkalinity in acidic, organic-rich freshwaters. Biogeosciences **12**: 67–68. doi:10.5194/bg-12-67-2015

Bates, R. G., and S. F. Acree. 1943. pH values of certain phosphate-chloride mixtures, and the second dissociation constant of phosphoric acid from 0 °C to 60 °C. J. Res. Natl. Bureau Stand. **30**: 129–155. doi:10.6028/jres.030.012

Bower, V. E., and R. G. Bates. 1955. pH values of the Clark and Lubs buffer solutions at 25 °C. J. Res. Natl. Bureau Stand. **55**: 197–200. doi:10.6028/jres.055.021

Butman, D., and P. A. Raymond. 2011. Significant efflux of carbon dioxide from streams and rivers in the United States. Nat. Geosci. **4**: 839–842. doi:10.1038/Ngeo1294

Byrne, R. H., and J. A. Breland. 1989. High precision multiwavelength pH determinations in seawater using cresol red. Deep-Sea Res Pt I. **36**: 803–810. doi:10.1016/0198-0149(89)90152-0

Chierici, M., A. Fransson, and L. G. Anderson. 1999. Influence of *m*-cresol purple indicator additions on the pH of seawater samples: Correction factors evaluated from a chemical speciation model. Mar. Chem. **65**: 281–290. doi:10.1016/S0304-4203(99)00020-1

Clayton, T. D., and R. H. Byrne. 1993. Spectrophotometric seawater pH measurements: Total hydrogen ion concentration scale calibration of m-cresol purple and at-sea results. Deep-Sea Res Pt I. **40**: 2115–2129. doi:10.1016/0967-0637(93)90048-8

Clayton, T. D., R. H. Byrne, J. A. Breland, R. A. Feely, F. J. Millero, D. M. Campbell, P. P. Murphy, and M. F. Lamb. 1995. The role of pH measurement in modern oceanic $CO_2$-system characterizations: Precision and thermodynamic consistency. Deep-Sea Res Pt II. **42**: 411–429. doi:10.1026/0967-0645(95)00028-O

Davison, W., and C. Woof. 1985. Performance tests for the measurement of pH with glass electrodes in low ionic-strength solutions including natural-waters. Anal. Chem. **57**: 2567–2570. doi:10.1021/ac00290a031

DeGrandpre, M. D., R. S. Spaulding, J. O. Newton, E. J. Jaqueth, S. E. Hamblock, A. A. Umansky, and K. E. Harris. 2014. Consideration for the measurement of spectrophotometric pH for ocean acidification and other studies. Limnol. Oceanogr.: Methods **12**: 830–839. doi:10.4319/lom.2014.12.830

Domenico, P. A., and F. W. Schwartz. 1990. Physical and chemical hydrogeology. Wiley.

Easley, R. A., and R. H. Byrne. 2012. Spectrophotometric calibration of pH electrodes in seawater using purified m-cresol purple. Environ. Sci. Technol. **46**: 5018–5024. doi:10.1021/es300491s

Finlay, K., R. J. Vogt, M. J. Bogard, B. Wissel, B. M. Tutolo, G. L. Simpson, and P. R. Leavitt. 2015. Reduction in $CO_2$ efflux from northern hardwater lakes with increasing atmospheric warming. Nature. **519**: 215–218. doi:10.1038/nature14172

French, C. R., J. J. Carr, E. M. Dougherty, L. A. K. Eidson, J. C. Reynolds, and M. D. DeGrandpre. 2002. Spectrophotometric pH measurements of freshwater. Anal. Chim. Acta. **453**: 13–20. doi:10.1016/S0003-2670(01)01509-4

Griffin, B. A., and J. J. Jurinak. 1973. Estimation of activity coefficients from the electrical conductivity of natural aquatic systems and soil extracts. Soil Sci. **116**: 26–30. doi:10.1097/00010694-197307000-00005

Harris, K. E. 2013. Applications of autonomous pH and $pCO_2$ sensors to study inorganic carbon dynamics in a coastal upwelling system. Ph.D. thesis. Univ. of Montana.

Liu, X., M. C. Patsavas, and R. H. Byrne. 2011. Purification and characterization of meta-cresol purple for spectrophotometric seawater pH measurements. Environ. Sci. Technol. **45**: 4862–4868. doi:10.1021/es200665d

Lynch, J. K. 2007. Characterization of riverine $CO_2$ cycles using direct, high-temporal resolution $pCO_2$ measurements. Master thesis. Univ. of Montana.

Lynch, J. K., C. M. Beatty, M. P. Seidel, L. J. Jungst, and M. D. DeGrandpre. 2010. Controls of riverine $CO_2$ over an annual cycle determined using direct, high temporal resolution $pCO_2$ measurements. J. Geophys. Res. Biogeosci. **115**: G03016. doi:10.1029/2009JG001132

Martz, T. R., J. J. Carr, C. R. French, and M. D. DeGrandpre. 2003. A Submersible autonomous sensor for spectrophotometric pH measurements of natural waters. Anal. Chem. **75**: 1844–1850. doi:10.1021/ac0205681

Millero, F. J. 2007. The marine inorganic carbon cycle. Chem. Rev. **107**: 308–341. doi:10.1021/cr0503557

Nimick, D. A., C. H. Gammons, and S. R. Parker. 2011. Diel biogeochemical processes and their effect on the aqueous chemistry of streams: A review. Chem. Geol. **283**: 3–17. doi:10.1016/j.chemgeo.2010.08.017

Pankow, J. F. 1991. Aquatic chemistry concepts, p. 638. CRC Press.

Patsavas, M. C., R. H. Byrne, and X. Liu. 2013. Purification of meta-cresol purple and cresol red by flash

chromatography: Procedures for ensuring accurate spectrophotometric seawater pH measurements. Mar. Chem. **150**: 19–24. doi:10.1016/j.marchem.2013.01.004

Raghuraman, B., G. Gustavson, O. C. Mullins, and P. Rabbito. 2006. Spectroscopic pH measurements for high temperatures, pressures and ionic strength. AIChE J. **52**: 3257–3265. doi:10.1002/aic.10933

Richards, L. A. 1954. Diagnosis and improvement of saline and alkali soils (Agriculture Handbook No. 60). United States Department of Agriculture.

Robert-Baldo, G. L., M. J. Morris, and R. H. Byrne. 1985. Spectrophotometric determination of seawater pH using phenol red. Anal. Chem. **57**: 2564–2567. doi:10.1021/ac00290a030

Seidel, M. P., M. D. DeGrandpre, and A. G. Dickson. 2008. A sensor for in situ indicator-based measurements of seawater pH. Mar. Chem. **109**: 18–28. doi:10.1016/j.marchem.2007.11.013

Spaulding, R. S., M. D. DeGrandpre, J. C. Beck, R. D. Hart, B. Peterson, E. H. De Carlo, P. S. Drupp, and T. R. Hammar. 2014. Autonomous in situ measurements of seawater alkalinity. Environ. Sci. Technol. **48**: 9573–9581. doi:10.1021/es501615x

Stauffer, R. E. 1990. Electrode pH error, seasonal epilimnetic $pCO_2$, and the recent acidification of the Maine lakes. Water Air Soil Pollut. **50**: 123–148. doi:10.1007/BF00284788

Talling, J. F. 2010. pH, the $CO_2$ system and freshwater science. Freshw. Rev. **3**: 133–146. doi:10.1608/FRJ-3.2.156

Wallin, M., I. Buffam, M. Öquist, H. Laudon, and K. Bishop. 2010. Temporal and spatial variability of dissolved inorganic carbon in a boreal stream network: Concentrations and downstream fluxes. J. Geophys. Res. **115**: G02014. doi:10.1029/2009jg001100

Yamazaki, H., R. P. Sperline, and H. Freiser. 1992. Spectrophotometric determination of pH and its application to determination of thermodynamic equilibrium constants. Anal. Chem. **64**: 2720–2725. doi:10.1021/ac00046a013

Yao, W., and R. H. Byrne. 2001. Spectrophotometric determination of freshwater pH using bromocresol purple and phenol red. Environ. Sci. Technol. **35**: 1197–1201. doi:10.1021/es001573e

Yao, W., X. Liu, and R. H. Byrne. 2007. Impurities in indicators used for spectrophotometric seawater pH measurements: Assessment and remedies. Mar. Chem. **107**: 167–172. doi:10.1016/j.marchem.2007.06.012

Yuan, S., and M. D. DeGrandpre. 2008. Evaluation of indicator-based pH measurements for freshwater over a wide range of buffer intensities. Environ. Sci. Technol. **42**: 6092–6099. doi:10.1021/es800829x

## Acknowledgments

This manuscript is presented in memory of Zachary Benson, a B.S. chemistry graduate of UM, who worked on this project as an undergraduate in its early stages. Zach passed away from complications due to leukemia in September 2008. Financial support was provided by the Montana University System Research Initiative (contract 51030-MUSRI2015-02), the M.J. Murdock Charitable Trust and the Montana Board of Research and Commercialization Technology. Undergraduate researchers (BW, TB, DC and EJ) were supported by the U.S. National Science Foundation under grants ARC-1107346 and OCE-1459255.

## Conflict of Interest

None declared.

*Submitted 14 June 2016*
*Revised 9 August 2016*
*Accepted 10 August 2016*

*Associate editor: John Smol*